J. Physiol. (1969), **204**, *pp.* 283–298
With 9 text-figures
Printed in Great Britain

VISIBILITY OF APERIODIC PATTERNS COMPARED WITH THAT OF SINUSOIDAL GRATINGS

BY F. W. CAMPBELL, R. H. S. CARPENTER AND J. Z. LEVINSON*

From the Physiological Laboratory, University of Cambridge

(*Received* 14 *August* 1968)

SUMMARY

1. Using experimental curves relating the threshold contrast of sinusoidal grating patterns to their spatial frequency, the expected threshold contrast curves for three aperiodic patterns, viz. a single half-cycle sinusoid bar, a single full-cycle sinusoid bar, and the boundary between an extended sinusoidal grating and a 50% grey surround, are calculated. In this calculation the assumption is made that the system is linear near the threshold.

2. Experiments are described in which the actual threshold contrast curves are determined for these aperiodic patterns by three observers. The patterns were generated on the face of an oscilloscope and could be varied in size and contrast.

3. These experimental curves agree well with the predictions in the high frequency region (i.e. above about 10 c/deg), but below this various complicating factors restrict the validity of the calculations.

4. Thus there is no reason to suppose that a linear theory cannot be used to predict visibility of aperiodic patterns near threshold.

INTRODUCTION

Recent studies aimed at elucidating the mechanisms involved in the transfer of spatial detail through the visual system have used as the input signal a grating pattern usually with a sinusoidal light distribution. Such patterns are physically appropriate for investigating the optical components of the visual system. Their use greatly simplifies the description and interpretation of the results (Campbell & Green, 1965). However, gratings have also been used as stimuli in investigations involving other visual elements, such as retinal ganglion cells (Enroth-Cugell & Robson,

* On leave from Bell Telephone Laboratories, Murray Hill, New Jersey, U.S.A.

1966), and the psychophysics of vision (Campbell & Robson, 1968). By breaking the system down to the dioptrics, the retinal and other peripheral neural elements, and a detection system, it is possible to discuss the properties of this cascade of elements using a common language derived from the application of grating stimuli. In this paper we attempt to relate quantitatively the thresholds for a variety of stimuli, although we restrict this choice to targets of luminance varying only in one dimension.

THEORY

Frequency characteristics, showing the sensitivity of the visual system for different spatial frequencies, may specify the system completely for the particular average luminance level at which the curve was obtained. In principle the visibility of any pattern may be predicted from the frequency characteristic: the success of such predictions will depend on whether or not the system is linear. In what follows, the visibility of several simple 'patterns' is predicted from the frequency characteristic for comparison with experimental results using those patterns.

The prediction is based on the fact that the line-spread function of the visual system may be found from the frequency characteristic. The line-spread function represents the spatial distribution of response (including both excitation and inhibition) as 'seen' by the threshold device to a stimulus consisting of an infinitesimally narrow straight line of unit intensity above (or below) background. If the sensitivity at frequency ν is represented by the function $S(\nu)$ then the line-spread function $\Lambda(x)$ representing the spread of excitation from a line to a point at a distance x from it is given by

$$\Lambda(x) = \int_{-\infty}^{+\infty} S(\nu) e^{i\Omega x} d\nu, \quad \Omega = 2\pi\nu. \tag{1}$$

For foveal vision we assume that there is no lateral displacement of the grating image at any frequency, i.e. it is symmetrical. In that case the imaginary part of eqn. (1) is zero and we may write

$$\Lambda(x) = 2\int_{0}^{\infty} S(\nu)\cos(\Omega x)\, d\nu. \tag{2}$$

Equation (2) lends itself to evaluation of Λ by computer. Evaluation by using the experimental values of $S(\nu)$ is possible, but less efficient than computation from an analytic approximation to S. From previous experiments (Campbell & Green, 1965) it appears that

$$S(\nu) = K(e^{-\alpha\Omega} - e^{\beta\Omega}) \tag{3}$$

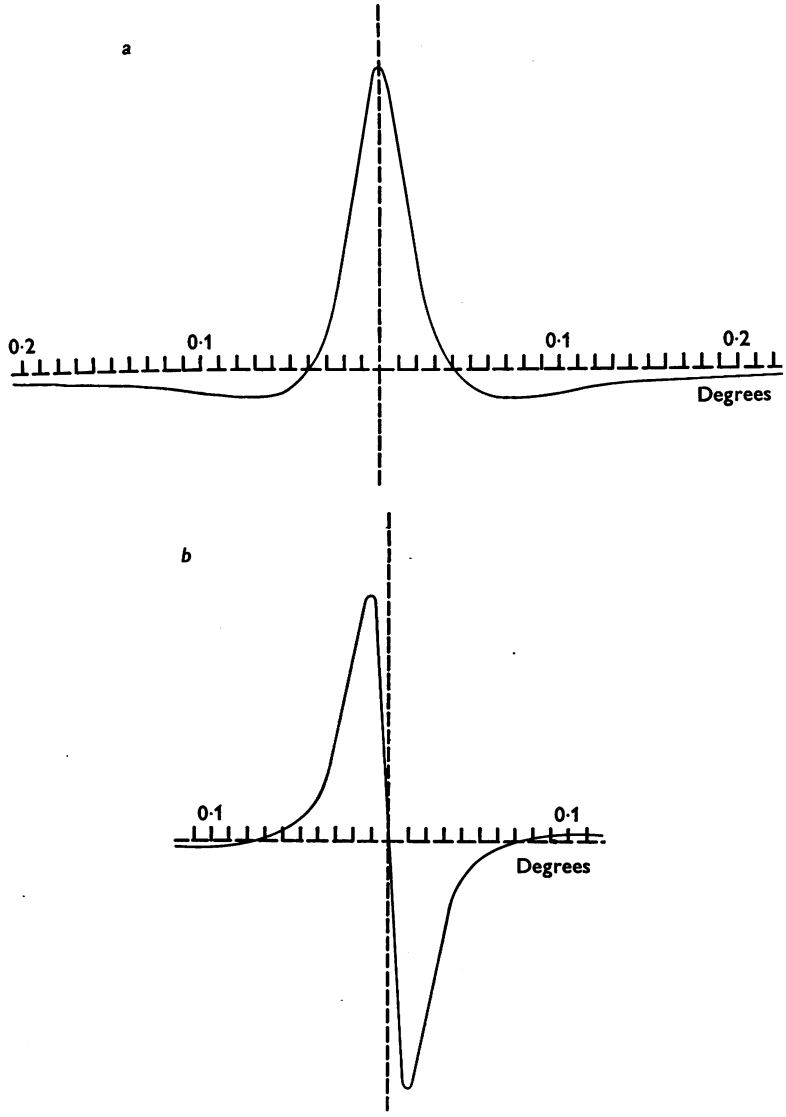

Fig. 1. (*a*) The line-spread function $\Lambda(x)$ computed from the data relating to the visibility of full gratings. The function is

$$\Lambda(x) = \frac{K}{\pi}\left(\frac{\alpha}{\alpha^2+x^2} - \frac{\beta}{\beta^2+x^2}\right).$$

Vertical scale arbitrary; horizontal scale in degrees.

(*b*) The derivative ($\Lambda'(x)$) of the line-spread function shown at (*a*). The function is

$$\Lambda'(x) = -\frac{2K}{\pi}\left(\frac{\alpha}{(\alpha^2+x^2)^2} - \frac{\beta}{(\beta^2+x^2)^2}\right).$$

Vertical scale arbitrary; horizontal scale in degrees.

provides a fit well within experimental error. Substituting eqn. (3) in eqn. (2) we obtain

$$\Lambda(x) = \frac{K}{\pi}\left(\frac{\alpha}{\alpha^2+x^2} - \frac{\beta}{\beta^2+x^2}\right). \tag{4}$$

The computed form of this line-spread function is shown in Fig. 1*a*. The two terms may be described respectively as excitatory and inhibitory, although the difference in sign between them is all that is meaningful. For small values of x (nearest the centre) the first term is the larger one, as α is smaller than β.

With the line-spread function (4) in hand, the response to any stimulus pattern, provided the pattern can be decomposed into a set of parallel straight lines, is easily computed (Fig. 2).

The visual response at x to a line at ξ of luminance modulation $L(\xi)$ and of width $\mathrm{d}\xi$ is then

$$\Lambda(x-\xi)\,L(\xi)\,\mathrm{d}\xi.$$

The total response at x to a stimulus of luminance $L(\xi)$ is

$$R(x) = \int_{-\infty}^{+\infty} \Lambda(x-\xi)\,L(\xi)\,\mathrm{d}\xi. \tag{5}$$

If stimulus luminance is that of a single bar generated by modulating otherwise uniform luminance sinusoidally for one half cycle (Fig. 3*b*), the modulation may be described as

$$L(\xi)\ a = \cos\Omega\xi, \quad \left(-\frac{1}{4\nu} \leqslant \xi \leqslant \frac{1}{4\nu}\right),$$

and $$L(\xi) = 0 \text{ elsewhere.}$$

Then

$$R(x) = a\int_{-\frac{1}{4\nu}}^{+\frac{1}{4\nu}} \Lambda(x-\xi)\cos(\Omega\xi)\,\mathrm{d}\xi. \tag{6}$$

If we assume that threshold modulation, a_T, is determined by the differences between the maximum and minimum responses (i.e. maximum and minimum values of R, β in Fig. 2), then these differences may be plotted as a function of the frequency of the sine wave of which one cycle provides the stimulus ($S_1(\nu)$ in Fig. 2).

Throughout this paper the frequency of non-periodic patterns will be used to mean the frequency of the periodic function used to generate them.

$R(x)$ for other stimuli may be computed in a similar way, for example for a 'double bar' generated in a similar way to the 'single bar' but extending over one whole cycle, or for the edge of a grating bounded by a uniform 50 % grey area. Figure 3 shows the luminance distribution across each of these types of stimuli.

A curve for the expected peak-to-trough differences for each of these three types of stimuli is plotted in Figs. 5–7, along with those for the grating frequency characteristic (3) from which the line-spread function was computed.

The evaluation of the convolution integral, eqn. (5), by computer may obscure insight into the processes it represents. It may be helpful to consider instead an approximation applicable at the high frequency

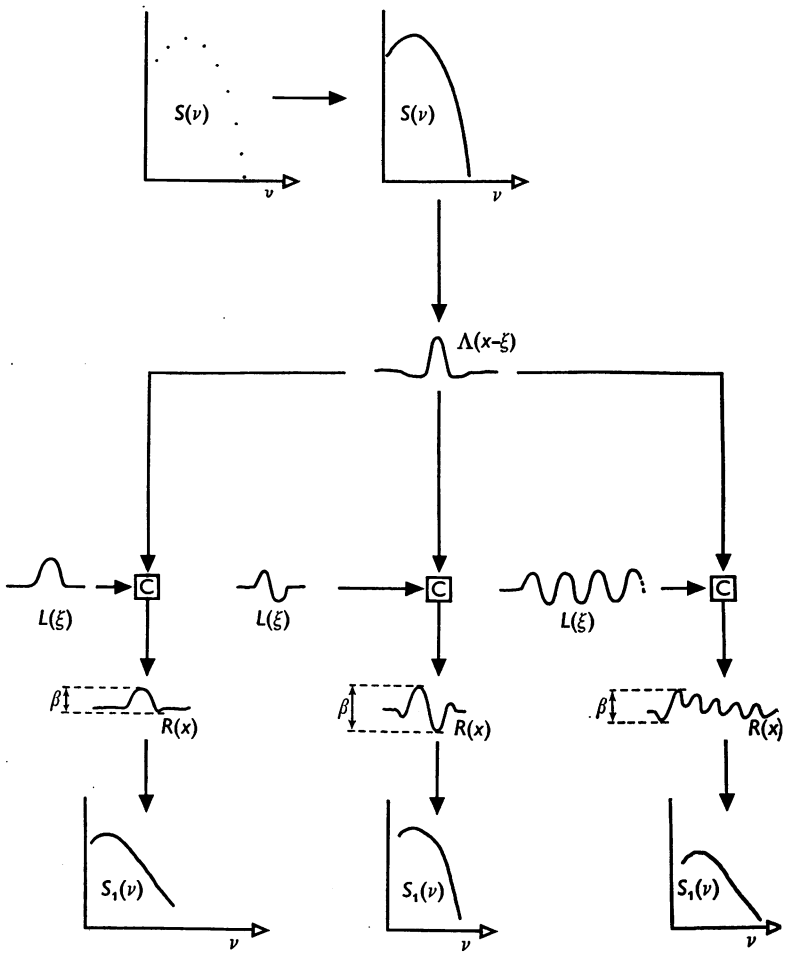

Fig. 2. The steps involved in computing the frequency response $S_1(\nu)$ to the three types of stimulus from that ($S(\nu)$) of a full grating. The first stage represents fitting the data for a full grating with a double exponential function, and the next represents computation of the associated line-spread function. C represents convolution, giving the response $R(x)$, of which the maximum peak-to-trough distance β is assumed constant at threshold.

portion of the curves. Consider, first, the visual response at a distance x from the centre of a half-sinusoid bar, as represented by eqn. (6). Integrating by parts,

$$R(x) = \frac{a}{\Omega}\left[(x-\xi)\sin\Omega\xi\right]_{-\frac{1}{4\nu}}^{\frac{1}{4\nu}} + \frac{a}{\Omega}\int_{-\frac{1}{4\nu}}^{\frac{1}{4\nu}} \Lambda'(x-\xi)\sin(\Omega\xi)\,d\xi$$

$$= \frac{a}{\Omega}\left[\Lambda\left(x-\frac{1}{4\nu}\right)+\Lambda\left(x+\frac{1}{4\nu}\right)\right] - \frac{a}{\Omega^2}\left[\Lambda'(x-\xi)\cos\Omega\xi\right]_{-\frac{1}{4\nu}}^{\frac{1}{4\nu}}$$

$$- \frac{a}{\Omega^2}\int_{-\frac{1}{4\nu}}^{\frac{1}{4\nu}} \Lambda''(x-\xi)\cos(\Omega\xi)\,d\xi$$

$$\approx 2a\left[\frac{\Lambda(x)}{\Omega} - \frac{\Lambda''(x)}{\Omega^3} + \ldots\right]. \tag{7}$$

In the above we have taken changes in $\Lambda(x)$ and its derivatives to be negligible over a distance $1/4\nu$ if ν is high enough. Under the same assumption all but the first term in (7) may be neglected. It represents the distribution of response at various distances x from a bar centred at $x = 0$, and of intensity $a/\pi\nu$ (the integrated intensity of a half-sinusoid of frequency ν and amplitude a); it is therefore to be expected that in the high frequency region threshold values of a will be proportional to ν. This is the equivalent of Ricco's law for narrow bars. Note, however, that the constant of proportionality is not arbitrary, the scale having been established by the grating data. The height of the single-bar curve relative to the grating curve is therefore significant. For example, if the threshold criterion were based on peak-to-mean-response difference rather than on peak-to-trough difference, the grating curve would have been a factor of two (roughly) lower relative to the single-bar curve than as drawn.

For the case of a 'double bar' (Fig. 3*c*), the stimulus may be described as

$$L(\xi) = a\sin\Omega\xi, \quad -\frac{1}{2\nu} \leqslant \xi \leqslant \frac{1}{2\nu} \quad \text{and} \quad L(\xi) = 0$$

everywhere else. Substituting in (5), and integrating by parts,

$$R(x) = a\int_{-\frac{1}{2\nu}}^{\frac{1}{2\nu}} \Lambda(x-\xi)\sin(\Omega\xi)\,d\xi$$

$$= \frac{a}{\Omega}\left[\Lambda(x-\xi)\cos\Omega\xi\right]_{-\frac{1}{2\nu}}^{\frac{1}{2\nu}} - \frac{a}{\Omega}\int_{-\frac{1}{2\nu}}^{\frac{1}{2\nu}} \Lambda'(x-\xi)\cos(\Omega\xi)\,d\xi$$

$$= \frac{a}{\Omega}\left\{\Lambda\left(x-\frac{1}{2\nu}\right) - \Lambda\left(x+\frac{1}{2\nu}\right)\right\} - \ldots$$

$$\approx -\frac{1}{\Omega\nu}\Lambda'(x) = -\frac{a}{2\pi\nu^2}\Lambda'(x). \tag{8}$$

At very high frequencies, then, the a_T versus ν curve is expected to become a straight line of slope 2 on a log–log plot. Note that the contrast scale factor is now not $\Lambda(x)$ but $\Lambda'(x)$. If the threshold for a single bar depends on the maximum value of the line-spread function, $\Lambda(0)$, then the threshold for a double bar depends on the extreme values of $\Lambda'(x)$ (of

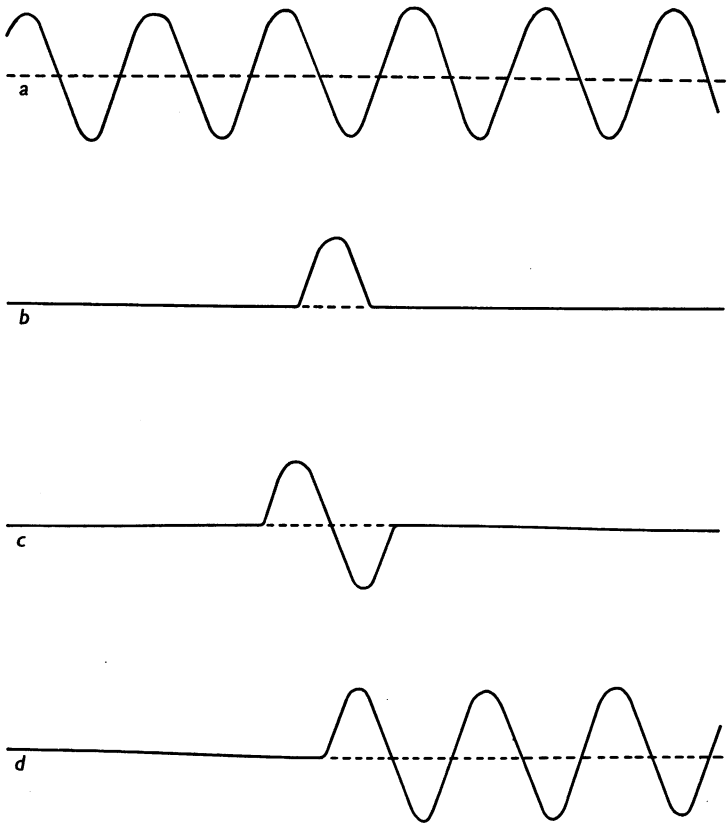

Fig. 3. Luminance (L) distribution across the test patterns used, all of the same frequency. (a) is grating; (b) is single bar; (c) is double bar; and (d) is the half grating beginning with bright half cycle. The mean luminance L_0 is indicated with a dashed line. The percentage contrast is given by 100 m, where $L = L_0 (1 + m \cos \Omega x)$.

which there are two, viz. a positive one to the left and a negative one to the right of the centre of the line-spread function: see Fig. 1b).

Finally, for a half grating (Fig. 3d), the interesting effect that the edge of the grating is visible when the grating itself is not, may be considered.

If we describe the modulation of the screen luminance by $L(\xi) = 0$ for $\xi < 0$, and $L(\xi) = a \sin \Omega\xi$ for $\xi \geqslant 0$ then eqn. (5) becomes

$$R(x) = a\int_0^\infty \Lambda(x-\xi)\sin\Omega\xi\,d\xi$$

$$= \left[-\frac{a}{\Omega}\Lambda(x-\xi)^\circ\cos\Omega\xi\right]_0^\infty - \frac{a}{\Omega}\int_0^\infty \Lambda'(x-\xi)\cos(\Omega\xi)\,d\xi.$$

For the upper limit $\Lambda(x-\xi)$ goes to zero, because we assumed our line-spread function to be of finite width. Similarly for subsequent terms. Then

$$R(x) = a\left\{\frac{\Lambda(x)}{\Omega} - \frac{\Lambda''(x)}{\Omega^3} + \ldots\right\}. \tag{9}$$

This is identical with eqn. (7), but for a factor of two. The edge of a grating should therefore look like a bar of half the intensity of a single half-sinusoid of the same frequency. The slope of the a_T versus ν curve will be 1, as for a single line. This relatively gentle slope is one reason why the edge of a grating may be seen at frequencies for which the grating itself has disappeared. The other necessary reason is that the peak value of the coefficient of the first term $\Lambda(0)$ is large enough. This puts the 'edge' sensitivity curve up into the region of practical contrasts.

METHODS

The test stimuli were generated on the face of an oscilloscope in the manner described in previous papers. The gratings, bars, etc. used as stimuli were always presented with the long axis vertical, and were kept accurately stationary on the screen. The modulation was continuously switched on and off so that the subject saw 1 sec of patterned and 1 sec of unpatterned screen of the same average luminance alternately throughout the experiments. Small marks were made on the screen to assist fixation. The screen was masked by a square white cardboard surround subtending 5° at the observer's eye, having a 1° diameter circular aperture cut in it. Its luminance was arranged to be equal to that of the oscilloscope screen, viewed binocularly at a distance of 200 in.

In most of the experiments the subject's task was to alter the attenuation of the signal modulating the luminance of the screen until he felt the visibility of the pattern was at threshold. In those experiments where frequency-of-seeing curves were desired, the experimenter controlled the attenuator and the subject reported whether or not he had a 1 sec presentation of the pattern initiated by himself and preceded and followed by unpatterned screen. Figure 4 shows the results of experiments to determine the quality of the pattern-generating system in terms of linearity and frequency response.

RESULTS

The data for subject RHSC in the case of the whole grating were fitted to the theoretical curve with no shift on the frequency axis, and the position on the contrast axis was chosen for the best fit for the grating and

single-bar data. The choice of position along the contrast axis is necessarily arbitrary since there is an arbitrary scale factor in the contrast equation. The space constant for subjects FWC and JZL were smaller than for RHSC by 30 % and 20 % respectively. These shifts were of course kept constant when comparing the theoretical predictions with experiment. Figure 5 shows the results obtained with all these subjects, shifted in this way, for full gratings and single bars. Figures 6 and 7 show similar results for double bars and half gratings, together with the full-grating curve for comparison.

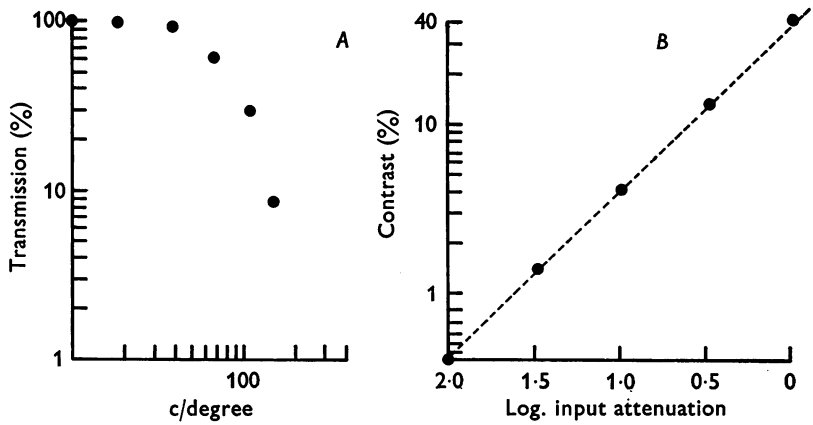

Fig. 4. (*A*) The spatial frequency response of the oscilloscope. Measurements were made by photo-electrically scanning the screen with the modulation voltage held constant. The spatial frequency of the sinusoidal gratings is expressed in c/degree as if viewed from a distance of 200 in from the screen. (*B*) The measured contrast of a grating pattern formed on the oscilloscope screen plotted against the attenuation of modulation voltage which was applied to the modulation grids of the cathode-ray tube. Measurements were made by scanning a 10 c/degree sinusoidal pattern with a linear photocell and narrow slit. The dashed line fitting the observations has a slope of 1.

The above conclusions allow direct comparison of theory with experiment in the high frequency region. This is the best region for comparison from the experimental point of view as well, because, at least for the edge effect, the determination of threshold in the low frequency region is confused by the visible presence of the grating itself, whereas, in the high frequency region, the threshold criterion for the edge and for a bar must be the same, no grating being visible in either case.

In any case we do not attach much significance to our data at frequencies below about 10 c/degree: in this region the interpretation of the results is confused, first by the limited size of the oscilloscope screen, and secondly

by the fact that the number of cycles visible is reduced. This latter has an effect that cannot adequately be predicted by an approach such as ours, as Nachmias (1968) has shown.

As can be seen from Fig. 5, the results for the single-bar thresholds fit a sensitivity curve with a slope of -1 in the high frequency region. It is only the integrated contrast of the line which determines its contrast threshold.

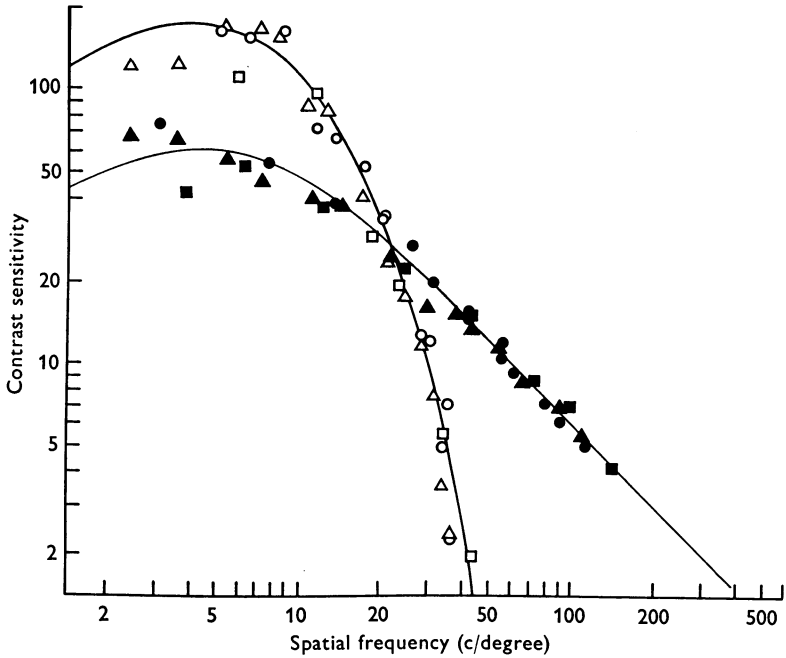

Fig. 5. The contrast sensitivity curves obtained for a full grating (○ △ □) and for a single bar (● ▲ ■) in the three subjects. The continuous lines through the results represent the theory. See text for the details of fitting.

If the oscilloscope had been capable of displaying bars thin enough and at unity contrast, the highest frequency which would have been detected would be at 500 c/degree. This extrapolated point is indicated in the frequency axis of Fig. 5. The maximum width at the base of such a bar is 3·6 sec. However, if the bar had had a rectangular profile the subtended angle at threshold would have been $\pi/2$ less (2·3 sec).

It will be noted that in Fig. 6 the results for a double bar consisting of a full sinusoid follow a slope of -2 as predicted by theory. However, there is a discrepancy of 0·1–0·15 log units in all subjects between the results and the computed theory. This discrepancy suggests that the threshold criterion assumed in the theory is unrealistic in this instance. Evidently the threshold criterion for a double bar is not based on the peak-to-trough contrast

criterion as we assumed for the grating results. On the other hand, a contrast criterion based on the peak-to-average (or on the trough-to-average) would have led to a curve which was displaced by 0·3 log units. Now, the double-bar response has two different troughs of different depths: perhaps the observer in practice compares the peak with the brightness sometimes on one side, sometimes on the other (B with A or C, Fig. 7). If such a strategy is being followed the average of the threshold settings may be

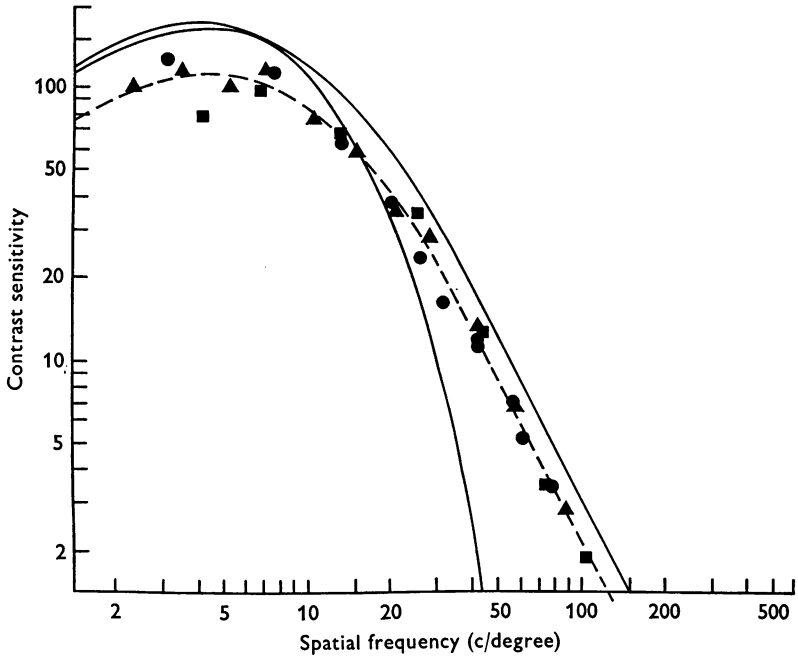

Fig. 6. The contrast sensitivity curve obtained (● ▲ ■) for double bars compared with theory (continuous line). Also displayed is the full grating curve as in Fig. 5. The dashed line is the theoretical curve lowered by 0·15 log units. For explanation, see text.

lower by some fraction of 0·3 log units. As the discrepancy is about 0·15 log units for all subjects, they may be comparing B with A or C with approximately equal probability. Other evidence in support of this interpretation is the finding that the S.D. of the double-bar readings are about 0·01 log units greater than those for the three other targets used in this study (see Table 1). This would be expected if the criterion had this additional variability in the case of the double-bar observations. Furthermore, the three subjects agreed that introspectively the double-bar thresholds were vaguer and more difficult.

Frequency-of-seeing curves were obtained for each subject and for each

pattern at certain frequencies. In no case was the 50% point of these curves significantly displaced from the threshold determined by the subject himself altering the contrast. This, we feel, provides some justification for the use of the subject-controlled threshold measurement in this case, since the time required to obtain a given standard *error* by this method is

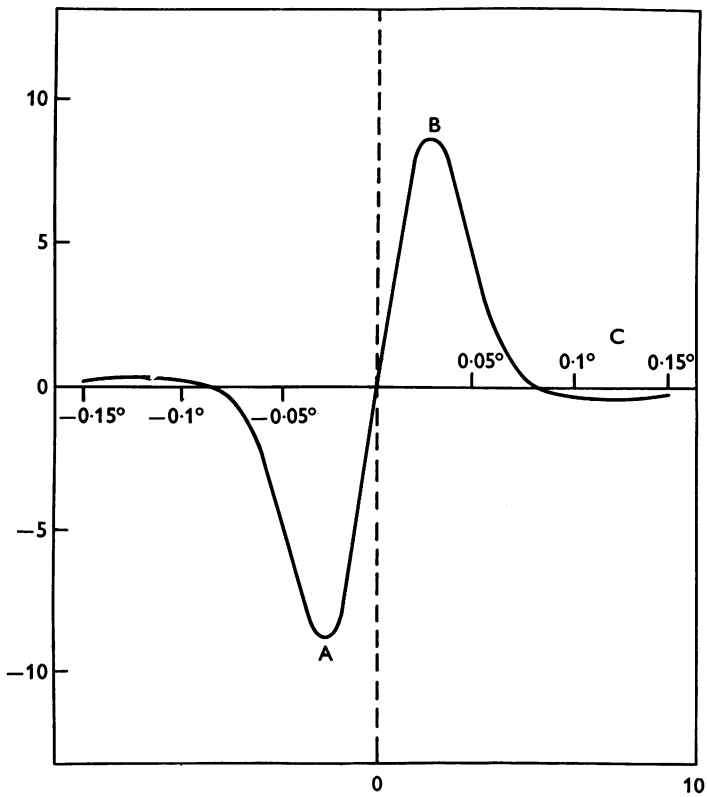

Fig. 7. Computed appearance of a double bar at 10 c/degree. Vertical axis arbitrary. For significance of A, B, C, see text.

TABLE 1. Mean S.D. in log units for all three subjects of observations of threshold contrast for the four different stimuli. The S.D.s are averaged over a set of four frequencies, viz. 20, 25, 30 and 35 c/degree

	Subject-controlled contrast	Frequency of seeing
Double bar	0·062	0·216
Full grating	0·051	0·097
Single bar	0·055	0·116
Half grating	0·050	0·102

about three times faster than by frequency-of-seeing measurements, and hence subjects could give more readings in a given time. The standard *deviation* of these estimates was consistently about twice that obtained by the latter method, except in the case of the double bar, in which it was about 3·5 times greater. This supports our suggestion about the singularity of the double-bar threshold.

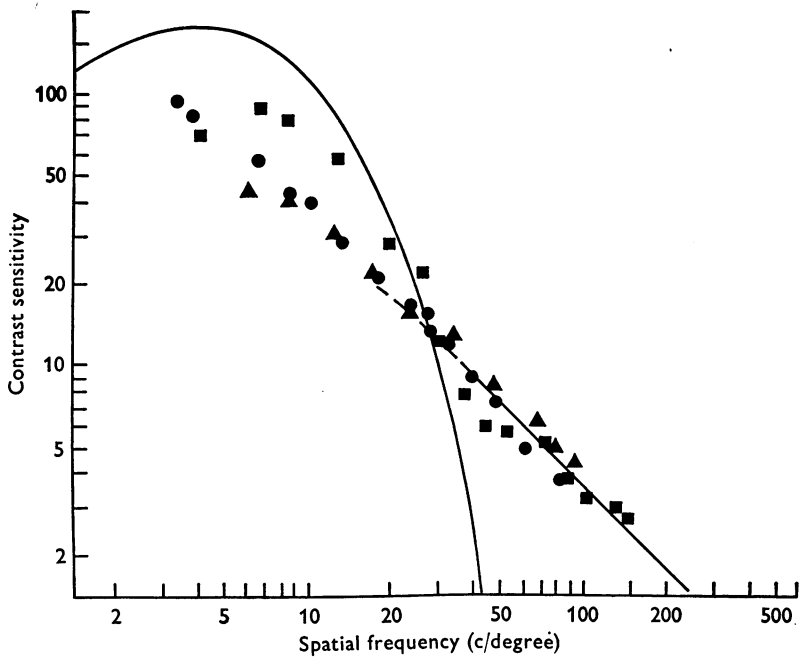

Fig. 8. Contrast sensitivity curves obtained for a half grating compared with theory (continuous line). Also displayed is the full-grating curve.

The results for the grating edge follow a slope of -1 in the high frequency region, as can be seen in Fig. 8. All three observers agree within experimental error in the high frequency region, but not so well in the low frequency region where the grating becomes as visible as the edge itself. The threshold criterion for the edge effect is unambiguous when the grating itself is not visible, i.e. one either sees a line at the edge, or not. However, when the grating is visible the decision as to whether the initial bar is brighter than the others may be based on a variety of criteria. Observer RHSC obtained edge thresholds much like grating thresholds at low frequencies. Apparently his threshold criterion amounted to disappearance of the bar at the edge. The other two observers apparently made some comparison between the brightness of the bar at the edge and that of

those in other portions of the field. FWC felt he ignored the rest of the grating, while JZL felt he compared the bar at the edge with the one next to it. We cannot put much stress on the results obtained at these low frequencies because it is difficult to predict them from the theory due to ambiguity in the assumptions which have to be made about the threshold criterion.

In the high frequency region the results for the edge are, on the average, 0·25 log units below those obtained for the single line presentation, while the theoretical prediction gives a value of 0·3 log units. This discrepancy seems to be real and not due to experimental error as we have re-measured it a number of times in the different subjects. We cannot account for it.

DISCUSSION

It may seem paradoxical that the edge of a grating may be visible when the body of the grating itself is not visible. The reader may satisfy himself about the phenomenon by viewing Fig. 9 from a distance of about 20 feet. He will then perceive the edge while not being able to resolve the grating proper. At closer distances the grating can be resolved.

Barlow (1965) has drawn attention to the artifact which can occur when moving gratings are vignetted by a rectangular aperture. His results show that a human observer can detect gratings above the diffraction limit by means of the flicker that appears at the edge of the aperture as each bar of a moving grating is occluded. Although his measurements were always made with moving gratings, he was aware that the effect could also occur with stationary gratings, for he states: 'For gratings only slightly below the ordinary resolution limit the edge effect is very prominent, and when the grating comes to rest one can often see, and correctly name, the dark or light bar of the grating next to the edge.'

In this attempt to account quantitatively for the thresholds of these different types of aperiodic patterns we make two assumptions: first, that the principle of superposition holds, that is, linear theory may be used, and, second, that a non-linear threshold mechanism is involved. In this model, whether or not the subject reports the presence of the stimulus depends only on the maximum peak-to-trough difference and not on the relative position of the peak and the trough concerned. Now this model is demonstrably false in the extreme case of two single bars of opposite contrast, separated by a considerable distance. However, our observations do not extend below a spatial frequency of about 3 c/degree and thus we cannot extend our predictions to patterns whose elements are separated by more than about 10 min. We must stress that this proposed simple mechanism only applies for higher spatial frequencies and clearly

other factors remain to be considered at low spatial frequencies (Nachmias, 1968).

Now, recent studies of the responses of the cells of the visual cortex of the cat (Campbell, Cooper & Enroth-Cugell, 1969) indicate that they are selectively sensitive to different bands of spatial frequency. Likewise, psychophysical studies in man suggest that there are channels selectively

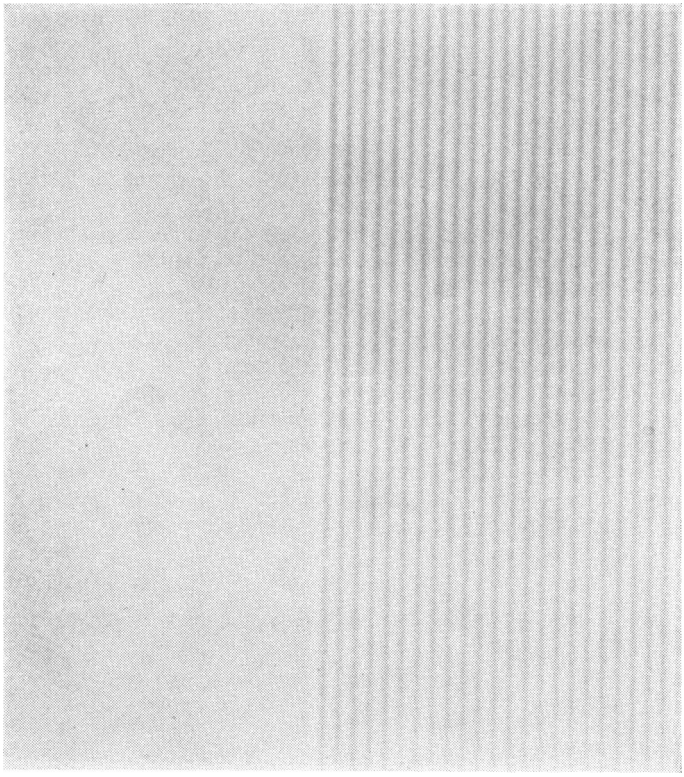

Fig. 9. Demonstration of the edge effect produced by the half-grating pattern. This is a photograph of the oscilloscope display actually used in the experiments. If viewed at a distance of about 20 feet the edge alone will be perceived but the grating itself will not be resolved.

sensitive to different bands covering a range of some four octaves of spatial frequency (Blakemore & Campbell, 1969). It might seem at first that these results are in conflict with the interpretation we are presenting here, which takes no account of the possible existence of such channels. However, a conflict will only arise if each channel has its own threshold device limiting the visibility of a particular pattern. If, on the other hand, the threshold device occurs after a 'pooling' of the outputs from the channels, then the

existence of the channels is irrelevant to the prediction of the visibility of aperiodic patterns from that of sinusoidal gratings. In such a case, we would predict that adapting to any one spatial frequency (Blakemore & Campbell, 1969) should make a much smaller change in the threshold of aperiodic patterns than has been observed for periodic patterns of the adapting frequency.

However, even if it transpires that thresholds are determined by one of many channels rather than by the system as a whole, there is no reason to believe that a linear theory of threshold visibility would have to be abandoned.

REFERENCES

BARLOW, H. B. (1965). Visual resolution and the diffraction limit. *Science, N.Y.* **149**, 553–555.

BLAKEMORE, C. & CAMPBELL, F. W. (1969). On the existence of neurones in the human visual system selectively sensitive to the orientation and size of retinal images. *J. Physiol.* **203**, 237–260.

CAMPBELL, F. W., COOPER, G. F. & ENROTH-CUGELL, CHRISTINA (1969). The spatial selectivity of the visual cells of the cat. *J. Physiol.* **203**, 223–235.

CAMPBELL, F. W. & GREEN, D. G. (1965). Optical and retinal factors affecting visual resolution. *J. Physiol.* **181**, 576–593.

CAMPBELL, F. W. & ROBSON, J. G. (1968). Application of Fourier analysis to the visibility of gratings. *J. Physiol.* **197**, 551–566.

ENROTH-CUGELL, CHRISTINA & ROBSON, J. G. (1966). The contrast sensitivity of retinal ganglion cells of the cat. *J. Physiol.* **187**, 517–552.

NACHMIAS, J. (1968). Visual resolution of two-bar patterns and square-wave gratings. *J. opt. Soc. Am.* **58**, 9–13.